

Ultra-Low Fire Glass-Free $\text{Li}_3\text{FeMo}_3\text{O}_{12}$ Microwave Dielectric Ceramics

Qingwei Liao, Yunli Wang, Feng Jiang, and Dong Guo[†]

Institute of Acoustics, Chinese Academy of Sciences, Beijing 100190, China

A new ultra-low fire glass-free microwave dielectric material $\text{Li}_3\text{FeMo}_3\text{O}_{12}$ was investigated for the first time. Single phase ceramics were obtained by the conventional solid-state route after sintering at 540°C–600°C. The atomic packing fraction, FWHM of the A_g oxygen-octahedron stretching Raman mode and Qf values of samples sintered at different temperatures correlated well with each other. The sample with a lower Raman shift showed a higher dielectric constant. Interestingly, the system also showed a distinct adjustable temperature coefficient of resonant frequency (from $-84 \times 10^{-6}/^\circ\text{C}$ to $25 \times 10^{-6}/^\circ\text{C}$).

I. Introduction

THE low temperature cofired ceramic (LTCC) technology has been used extensively for the fabrication of high-performance microelectronic packages due to its durability, compactness, and manufacturability. The LTCC technology is especially useful for microwave application. Recently, a great deal of effort has been made to fabricate low temperature sinterable microwave dielectric ceramics with a wide range of dielectric constant (ϵ_r), a high quality factor (Qf), and an adjustable temperature coefficient of resonant frequency (τ_f).¹ However, at present reducing the sintering temperature without affecting the electrical performance is still a challenge. The commonly used methods to reduce the sintering temperature, including low melting glass addition, chemical processing, and use of fine raw materials,^{2,3} usually lead to complicated fabrication procedure and deteriorated properties. Recent studies showed that the compound with low-melting temperature oxides, such as TeO_2 (733°C), MoO_3 (795°C), Bi_2O_3 (817°C), and Li_2CO_3 (723°C) etc., could give rise to a low or even ultra-low sintering temperature.^{4–10} While without glass addition, it is still hard to lower the sintering temperature below 900°C. Exceptions are the molybdate and tellurate, which can be densified below 750°C.^{6–10} Tellurate, like $\text{Zn}_3\text{Te}_3\text{O}_8$ - TiTe_3O_8 , CaTe_2O_5 - TeO_2 and SrTe_2O_5 - TeO_2 , were reported to have a sintering temperature in the range of about 600°C–650°C. Nevertheless, they still show good electric properties with a dielectric constant ϵ_r of about 19.8–28.7, a Qf value in the range of 12 000–50 000 GHz, and a τ_f in the range of about $-3.8 \times 10^{-6}/^\circ\text{C}$ – $3.0 \times 10^{-6}/^\circ\text{C}$.^{11,12} However, TeO_2 has the problems of high cost and toxicity. In contrast, molybdate is much more advantageous for practical use in LTCC microwave components. Typical molybdate like $\text{Li}_2(\text{M}^{2+})_2\text{Mo}_3\text{O}_{12}$ and $\text{Li}_3(\text{M}^{3+})\text{Mo}_3\text{O}_{12}$ ($\text{M}=\text{Zn}$, Ca , Al , and In) were reported to have relatively high Qf values (36 000–70 000 GHz) and a

low sintering temperature (570°C–630°C), but their τ_f is still large ($-90 \times 10^{-6}/^\circ\text{C}$ – $-73 \times 10^{-6}/^\circ\text{C}$).⁶ Here, we report a new microwave dielectric material $\text{Li}_3(\text{M}^{3+})\text{Mo}_3\text{O}_{12}$ ($\text{M}=\text{Fe}$) that have ultra-low sintering temperature (540°C–600°C) with adjustable τ_f ($-84 \times 10^{-6}/^\circ\text{C}$ – $24 \times 10^{-6}/^\circ\text{C}$). The crystal structure, Raman scattering spectra, and dielectric properties of the material were investigated.

II. Experimental Procedure

The $\text{Li}_3\text{FeMo}_3\text{O}_{12}$ ceramics were prepared by the solid-state method. High-purity (>99.9%) Li_2CO_3 , Fe_2O_3 and MoO_3 raw materials were ball-milled using de-ionized water as the medium for 10 h. The dried powders were calcined (500°C for 3 h), ground, and pressed into pellets. After sintering at 540°C–600°C for 6 h, ceramic samples with a diameter of 10 mm and a thickness of 5 mm were obtained. The phase structure was examined by XRD (D8; Bruker, Stuttgart, Germany). The morphology of the fractured surfaces of the samples was examined by a Scanning Electron Microscope (S-4800; Hitachi, Tokyo, Japan). Microwave dielectric properties were measured by a network analyzer (8720ES; Agilent, Santa Clara, CA) in the frequency range of 12.0–14.5 GHz. The dielectric constant was measured by the Hakki-Coleman method, as modified by Courtney,¹³ and the unloaded Q values were measured by the cavity method.¹⁴ The τ_f values were determined from the resonant frequencies in the temperatures range of 25°C–85°C. The measurement error of dielectric constant, τ_f and Qf were less than 0.5% $\times \epsilon_r$, $0.5 \times 10^{-6}/^\circ\text{C} \times \tau_f$ and 5% $\times Qf$, respectively.

III. Results and Discussion

The XRD patterns of the $\text{Li}_3\text{FeMo}_3\text{O}_{12}$ samples shown in Fig. 1 indicate that single orthorhombic phase structure (ICSD: 16176) was obtained in all the temperatures. Such a structure belongs to the space group $Pnma$ (D_{2h}^{16}) and contains four $\text{Li}_3\text{FeMo}_3\text{O}_{12}$ molecules per primitive cell. From the schematic illustration of the $\text{Li}_3\text{FeMo}_3\text{O}_{12}$ supercell ($4 \times 4 \times 4$) in the inset of Fig. 1, we can see that the $\text{Li}_3\text{FeMo}_3\text{O}_{12}$ lattice consists of edge/corner shared Li/FeO₆ octahedra and MoO₄ tetrahedra. Each unit contains one central Li/FeO₆ octahedron surrounded by six corner-shared MoO₄ tetrahedra, which are in turn connected with twelve edge-shared peripheral Li/Fe octahedra. The lattice parameters calculated from the XRD patterns are listed in Table I, from which the theoretical density¹⁵ and packing fraction can be calculated. As shown in Fig. 2, the density increases with increasing sintering temperature. The relatively density (> 95%) indicates that the $\text{Li}_3\text{FeMo}_3\text{O}_{12}$ ceramics can be densified at 540°C. The inset of Fig. 2 is a SEM image of a typical sample (600°C), which consists of rod-shaped grains with a diameter of 0.5–1 μm and a length of 2–2.5 μm . Other samples have a similar morphology.

Figure 3 Shows the Raman spectra of different $\text{Li}_3\text{FeMo}_3\text{O}_{12}$ samples. The material has 76 atoms in its unit cell (see the inset of Fig. 1), which give rise to 228 spectrum

D. Johnson—contributing editor

Manuscript No. 34486. Received January 29, 2014; approved May 23, 2014.

[†]Author to whom correspondence should be addressed. e-mail: dong.guo@mail.ioa.ac.cn

Table I. Crystallographic Data of $\text{Li}_3\text{FeMo}_3\text{O}_{12}$ Microwave Dielectric Ceramics

Sintering temperature (°C)	Lattice parameters (Å)			Vol (Å^3)
	<i>a</i>	<i>b</i>	<i>c</i>	
540	17.58797	10.48384	5.09483	939.43
560	17.64741	10.4613	5.08227	938.26
580	17.57049	10.47891	5.09788	938.62
600	17.57880	10.47976	5.09721	939.02

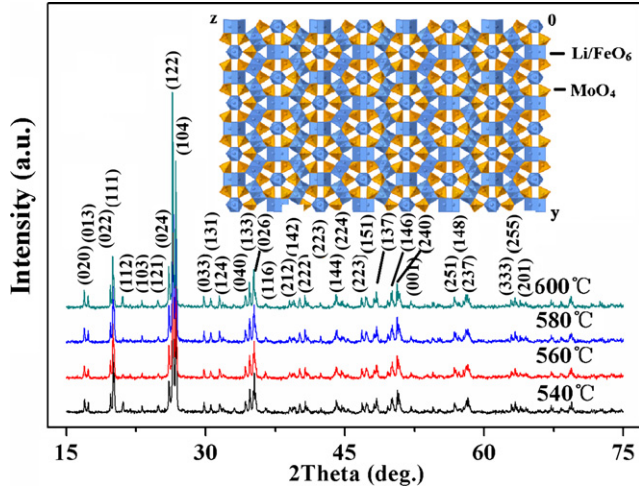


Fig. 1. The XRD patterns of the $\text{Li}_3\text{FeMo}_3\text{O}_{12}$ ceramics after sintering at 540°C ~ 600°C. The inset shows the (4 × 4 × 4) supercell of the lattice, where the blue and yellow parts represent Li/FeO₆ octahedron and MoO₄ tetrahedron, respectively.

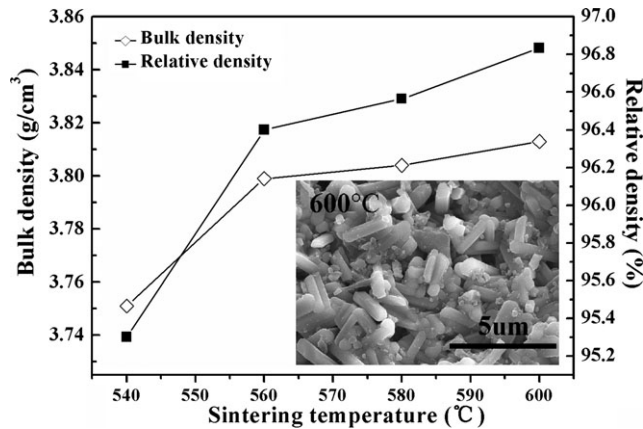


Fig. 2. The bulk density and relative density of the $\text{Li}_3\text{FeMo}_3\text{O}_{12}$ ceramics as a function of sintering temperature. The inset shows the SEM photograph of a typical sample that has been sintered at 600°C.

branches. Using the group theoretical method,¹⁶ and via the irreducible representations for the lattice, the Raman active modes can be calculated as $\Gamma_{\text{Raman}} = 5A_g + 4B_{1g} + 5B_{2g} + 4B_{3g}$ (Γ_{Raman} is the irreducible representation). Previous studies have shown that the A_g mode scattering, which is related to the stretching vibrations of the oxygen octahedron, are closely related to the microwave dielectric properties.^{17,18} The A_g mode scattering always has a high scattering frequency and strong intensity.^{17,18} Therefore, the strongest peak around 933 cm^{-1} is assigned to the A_g mode scattering, which will be discussed in the following.

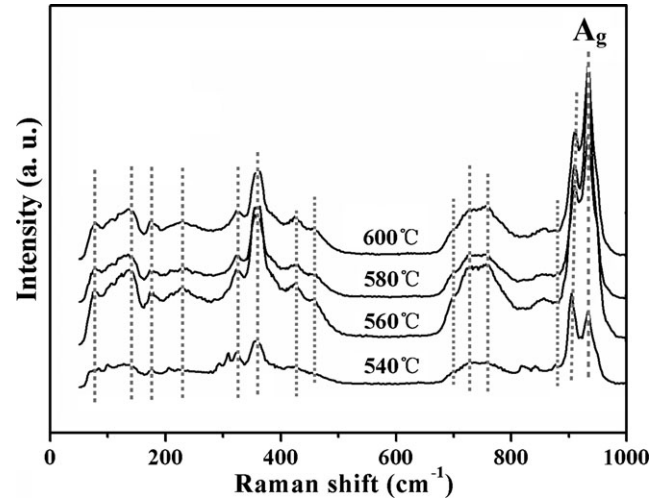


Fig. 3. The Raman scattering spectra of the $\text{Li}_3\text{FeMo}_3\text{O}_{12}$ ceramics after sintering at 540°C ~ 600°C. The main Raman active vibrational modes are marked by the dash lines.

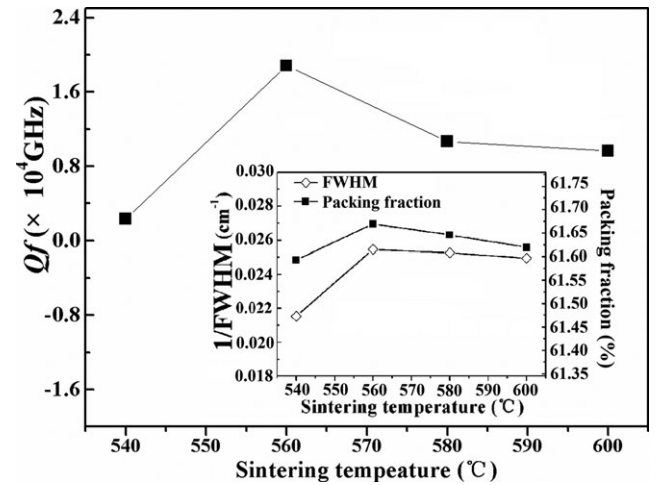


Fig. 4. The Qf value of the $\text{Li}_3\text{FeMo}_3\text{O}_{12}$ ceramics as a function of sintering temperature. The inset shows the packing fraction and 1/FWHM of the A_g mode Raman scattering peak of different ceramic samples.

As an important structural parameter, the packing fraction (the summation of the volume of packed ions over the volume of a primitive unit cell) has a strong influence on the dielectric properties, which could be obtained from Eq. (1):¹⁹

$$\begin{aligned} \text{packing fraction (\%)} &= \frac{\text{volume of the atoms in the cell}}{\text{volume of primitive unit cell}} \\ &= \frac{\text{volume of the atoms in the cell}}{\text{volume of unit cell}} \times Z \end{aligned} \quad (1)$$

where Z is the number of formula units per unit cell. As shown in the inset of Fig. 4, the packing fraction increases from 61.5930% to 61.6697% when the sintering temperature is increased from 540°C to 560°C, and then it decreases to 61.6198% when the temperature is further increased to 600°C.

The inverse of the FWHM (Full Width at Half Maximum) of the A_g mode of the Raman peak, the packing fraction, and Qf values of different $\text{Li}_3\text{FeMo}_3\text{O}_{12}$ ceramic samples are shown in Fig. 4. A rather good correlation among the data can be clearly seen. Namely, all three parameters reach maximum values at 560°C and then decreases slightly with further

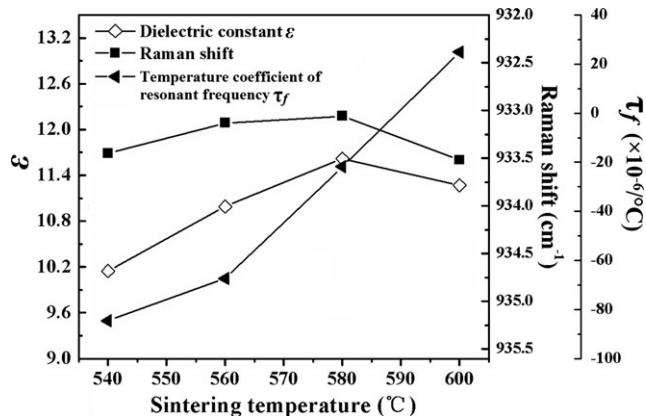


Fig. 5. The dielectric constant ϵ_r , the A_g mode Raman shift and the temperature coefficient of resonant frequency τ_f of different $\text{Li}_3\text{FeMo}_3\text{O}_{12}$ ceramics samples.

increasing of temperature. The Qf value is related to the dielectric loss from anharmonic vibrations of the atoms.²⁰ The increase in packing fraction means a decreased vibration space, and this in turn may give rise to a decrease in anharmonic vibration. Consequently, a good correlation between Qf and packing fraction is observed. The decrease in the $1/\text{FWHM}$ of the A_g mode reflects a decreased anharmonicity. The anharmonicity of the vibration is related to the phonon damping²¹ and in turn to the intrinsic dielectric loss. Therefore, the narrowing of FWHM of the A_g mode peak implies a larger damping and dielectric loss, and hence a lower Qf value is observed.

The correlation between Raman shift and the dielectric constant ϵ_r , as well as the temperature coefficient of resonant frequency τ_f are shown in Fig. 5. A lower Raman shift implies a more rigid oxygen octahedron and a lower polarizability, and this in turn results in a lower ϵ_r . Therefore, the Raman shift and ϵ_r show a good correlation. An interesting phenomenon reflected from Fig. 5 is that, with the increase in the sintering temperature, the τ_f value varies almost linearly from $-84.5912 \times 10^{-6}/^\circ\text{C}$ to $24.8967 \times 10^{-6}/^\circ\text{C}$. This implies that the new $\text{Li}_3\text{FeMo}_3\text{O}_{12}$ system has distinct adjustable microwave performance. This character may be used to meet specific requirements of a certain devices and can be achieved by controlling the sintering temperature. This is probably related to the specific crystal structure of $\text{Li}_3\text{FeMo}_3\text{O}_{12}$. The underlying mechanism deserves further investigation.

IV. Conclusions

The crystal structure, Raman scattering spectra and microwave dielectric properties of a new $\text{Li}_3\text{FeMo}_3\text{O}_{12}$ microwave dielectric material were investigated. The results showed that the $\text{Li}_3\text{FeMo}_3\text{O}_{12}$ ceramics could be densified at 540°C . The packing fraction, FWHM of the Raman A_g mode and Qf value of samples sintered at different temperatures correlated well with each other. Also, the sample with a lower Raman shift showed a higher dielectric constant. The new system also exhibits a distinct adjustable temperature coefficient of resonant frequency that can be controlled by sintering temperature.

Acknowledgment

This work was supported by the 'Bairen Program' of Chinese Academy of Sciences and the National Key Basic Research Program of China (973 Program, grant no. 2013CB632900). The authors also thank the Open Foundation of the State Key Laboratory of New Ceramics and Fine Processing of Tsinghua University.

References

- M. T. Sebastian and H. Jantunen, "Low Loss Dielectric Materials for LTCC Applications: A Review," *Int. Mater. Rev.*, **53**, 57–90 (2008).
- T. Takada, S. F. Wang, S. Yoshikawa, S. J. Jang, and R. E. Newnham, "Effect of Glass Additions on $\text{BaO-TiO}_2\text{-WO}_3$ Microwave Ceramics," *J. Am. Ceram. Soc.*, **24**, 1799–803 (2004).
- S. Hirano, T. Hayashi, and A. Hattori, "Chemical Processing and Microwave Characteristics of $(\text{Zr},\text{Sn})\text{TiO}_4$ Microwave Dielectrics," *J. Am. Ceram. Soc.*, **74** [6] 1320–4 (1991).
- Q. Zeng, W. Li, J. I. Shi, and J. K. Guo, "A new $\text{Li}_2\text{O-Nb}_2\text{O}_5\text{-TiO}_2$ Microwave Dielectric Ceramic Composite," *Phys. Status Solidi A*, **203** [11] R91–3 (2006).
- N. Wang, M. Zhao, W. Li, and Z. Yin, "The Sintering Behavior and Microwave Dielectric Properties of $\text{Bi}(\text{Nb},\text{Sb})\text{O}_4$ Ceramics," *Ceram. Int.*, **30** [6] 1017–22 (2004).
- D. Zhou, C. A. Randall, L. Pang, H. Wang, X. Wu, J. Guo, G. Zhang, L. Shui, and X. Yao, "Microwave Dielectric Properties of $\text{Li}_2(\text{M}^{2+})_2\text{Mo}_3\text{O}_{12}$ and $\text{Li}_3(\text{M}^{3+})\text{Mo}_3\text{O}_{12}$ ($\text{M}=\text{Zn}, \text{Ca}, \text{Al}, \text{In}$) Lyonsite-Related-Type Ceramics With Ultra-Low Sintering Temperature," *J. Am. Ceram. Soc.*, **94** [3] 802–5 (2011).
- L. Pang, D. Zhou, C. L. Cai, and W. Liu, "Infrared Spectroscopy and Microwave Dielectric Properties of Ultra-low Temperature Firing $(\text{K}_{0.5}\text{La}_{0.5})\text{Mo}_4$ Ceramics," *Mater. Lett.*, **92**, 36–8 (2013).
- D. Zhou, C. A. Randall, L. Pang, H. Wang, J. Guo, G. Zhang, Y. WU, K. T. Guo, L. Shui, and X. Yao, "Microwave Dielectric Properties of $(\text{ABi})_1/2\text{MoO}_4$ ($\text{A}=\text{Li}, \text{Na}, \text{K}, \text{Rb}, \text{Ag}$) Type Ceramics With Ultra-low Firing Temperatures," *Mater. Chem. Phys.*, **129**, 688–92 (2011).
- S. F. Wang, S. J. Wang, Y. R. Wang, Y. F. Hsu, L. Y. Chen, and J. S. Tsai, "Effect of SiO_2 Addition on the Microstructure and Microwave Dielectric Properties of Ultra-low Fire TiTe_3O_8 Ceramics," *Ceram. Int.*, **35**, 1813–7 (2009).
- D. K. Kwon, M. T. Lanagan, and T. R., "Shrout. Microwave Dielectric Properties of BaO-TeO_2 Binary Compounds," *Mater. Lett.*, **61**, 1827–31 (2007).
- S. F. Wang and Y. F. Hsu, "Ultra-low-Fire $\text{Zn}_2\text{Te}_3\text{O}_8\text{-TiTe}_3\text{O}_8$ Ceramic Composites," *J. Am. Ceram. Soc.*, **94** [3] 812–6 (2011).
- S. F. Wang, "Effects of CaTiO_3 and SrTiO_3 Additions on the Microstructure and Microwave Dielectric Properties of Ultra-low Fire TeO_2 Ceramics," *J. Am. Ceram. Soc.*, **93** [10] 3272–7 (2010).
- W. E. Courtney, "Analysis and Evaluation of a Method of Measuring the Complex Permittivity and Permeability of Microwave Insulators," *IEEE Trans. Microw. Theory Tech.*, **18** [8] 476–85 (1970).
- D. Kajfež, S. Chebolu, M. R. Abdul-Gaffoor, and A. A. Kishk "Uncertainty Analysis of the Transmission-Type Measurement of Q-Factor," *IEEE Trans. Microw. Theory Tech.*, **47** [3] 367–71 (1999).
- Q. Liao, L. Li, X. Ren, and X. Ding, "New Low-Loss Microwave Dielectric Material ZnTiNbTaO_8 ," *J. Am. Ceram. Soc.*, **94** [10] 3237–40 (2011).
- Q. Liao and L. Li, "Structural Dependence of Microwave Dielectric Properties of Ixolite Structured $\text{ZnTiNb}_2\text{O}_8$ Materials: Crystal Structure Refinement and Raman Spectra Study," *Dalton Trans.*, **41** [23] 6963–9 (2012).
- M. Y. Chen, C. T. Chia, I. N. Lin, L. J. Lin, C. W. Ahn, and S. Nahm, "Microwave Properties of $\text{Ba}(\text{Mg}_{1/3}\text{Ta}_{2/3})\text{O}_3$, $\text{Ba}(\text{Mg}_{1/3}\text{Nb}_{2/3})\text{O}_3$ and $\text{Ba}(\text{Co}_{1/3}\text{Nb}_{2/3})\text{O}_3$ Ceramics Revealed by Raman Scattering," *J. Eur. Ceram. Soc.*, **26**, 1965–8 (2006).
- M. S. Fu, X. Q. Liu, and X. M. Chen, "Raman Spectra Analysis for $\text{Ca}(\text{B}'_{1/3}\text{B}''_{2/3})\text{O}_3$ Based Complex Perovskite Ceramics," *J. Appl. Phys.*, **104**, 104108 (2008).
- E. S. Kim, B. S. Chun, R. Freer, and R. J. Cernik, "Effects of Packing Fraction and Bond Valence on Microwave Dielectric Properties of $\text{A}^{2+}\text{B}^{6+}\text{O}_4$ ($\text{A}^{2+}:\text{Ca}, \text{Pb}, \text{Ba}; \text{B}^{6+}:\text{Mo}, \text{W}$) Ceramics," *J. Eur. Ceram. Soc.*, **30**, 1731–6 (2010).
- V. L. Gurevich and A. K. Tagantsev, "Intrinsic Dielectric Loss in Crystals," *Adv. Phys.*, **40** [6] 719–67 (1991).
- Y. C. Chen, H. F. Cheng, H. L. Liu, C. T. Chia, and I. N. Lin, "Correlation of Microwave Dielectric Properties and Normal Vibration Modes of $\text{xBa}(\text{Mg}_{1/3}\text{Ta}_{2/3})\text{O}_3\text{-(1-x)}\text{Ba}(\text{Mg}_{1/3}\text{Nb}_{2/3})\text{O}_3$ Ceramics: II. Infrared Spectroscopy," *J. Appl. Phys.*, **94** [5] 3365–70 (2003). □